A Novel Heuristic Data Routing for Urban Vehicular Ad-hoc Networks

Ammar Hawbani, Xingfu Wang, Ahmed Dubai, Liang Zhao, Omar Busaileh, Ping Liu, and Mohammed A. A. Al-qaness

Abstract— This work is devoted to solving the problem of multi-criteria multi-hop routing in vehicular ad-hoc networks (VANETs), aiming at three goals, increasing the end-to-end delivery ratio, reducing the end-to-end latency, and minimizing the network overhead. To this end and beyond the state-of-the-art, **HE**uristic **RO**uting for Vehicular Networks (HERO), which is a distributed routing protocol for urban environments, encapsulating two main components, is proposed. The first component, road-segment selection, aims to prioritize the road segments based on a heuristic function that contains two probability distributions, namely, shortest distance distribution (SDD) and connectivity distribution (CD). The mass function of SDD is the product of three quantities, the perpendicular distance, the dot-production angle, and the segment length. On the other hand, the mass function of CD considers two quantities, the density of vehicles and the inter-distance of vehicles on the road segment. The second component, vehicle selection, aims to prioritize the vehicles on the road segment based on four quantities, the relative speed, the movement direction, the available buffer size, and the signal fading. The simulation results showed that HERO achieved a promising performance in terms of delivery success ratio, delivery delay, and communication overhead.

Index Terms: Heuristic routing, probabilistic routing, intelligent transportation systems, vehicular ad hoc networks

1. Introduction

Vehicular communication can play a critical role in permitting numerous applications such as traffic control, collision avoidance, and lane change assistance in *Intelligent Transportation Systems* (ITS) [1]. This communication paradigm paves the way for many applications to realize the future of ultimately autonomous driving. Indeed, efficient vehicular networking is fundamental to a wide range of applications in road safety, business, infotainment, and smart cities [2] [3]. Generally, VANETs consist of a limited number of vehicles, each equipped with an *onboard unit* (OBU) together with GPS and street-level *digital maps*. OBU enables inter-vehicle communication, *vehicle-to-vehicle* (V2V), as well as communication between *roadside units* (RSUs) and vehicles, sometimes named *vehicle to infrastructure* (V2I). In particular, fewer RSUs are deployed to facilitate cost-effective vehicular communication [4]. Nevertheless, RSUs are still not yet widely available and have experienced a very slow pace of implementation due to their expensive cost [5]. RSUs installation and placement strategies are studied in [6], [7], and [8].

The mainstay for implementing ITS applications is the multi-hop routing mechanism, which should guarantee the quality of services such as higher packet delivery ratio, lower latency, and smaller overhead. Multi-hop routing is an appropriate mechanism to disseminate data in such mobile-nodes networks [9], [10], [11]. In such a mechanism, the determination of a set of road segments and a set of relay vehicles is the main research issue [12]. The process of selecting a set of road segments is called *inter-routing*, while the process of selecting a set of relay vehicles is called *intra-routing*. Both *inter-routing* and *intra-routing* employ different routing criteria that mostly characterize the quality of the selected path between source and destination vehicles. Shortest distance and density are the frequent criteria that have been used to estimate the quality of *inter-routing*, while speed and direction are usually employed to characterize the *intra-routing*. Although the multi-hop routing for mobile environments has been extensively investigated in the context of MANET (*Mobile Ad hoc Network*) [13], the vehicular network has obvious features making the routing mechanism in MANET no longer suitable. VANET possesses unique characteristics such as energy is no longer an issue, and nodes have higher mobility in restricted streets.

Problem and Motivations: The network layer performance in VANETs is conjointly influenced by multiple quantities (i.e., criteria) such as vehicle's speed, signal fading, direction angle between the source and next-hop vehicles, the shortest distance from source to destination, communication range, road size (i.e., number of lanes), segment length, segment connectivity, etc. Previous works considered few criteria during the selection of forwarder vehicles or road segments. For example, the authors in [14] prioritize the next-hop forwarders based on vehicle's movement similarity by considering two quantities, the speed and the movement direction. In contrast, the authors in [15] prioritize the next-hop forwarders based on the shortest distance to the next-hop junction. More quantities and examples are explained in Section 2. Such limited

- *Ammar H., Xingfu W. {anmande, wangxfu} @ustc.edu.cn, Omar B. and Ping L. {busaileh, iacmy }@mail.ustc.edu.cn are with School of Computer Science and Technology; University of Science and Technology of China, Hefei, Anhui 230027, China;*
- *Ahmed Al-Dubai (a.al-dubai@napier.ac.uk) is with School of Computing; Edinburgh Napier University;*
- *Liang Zhao (lzhao@sau.edu.cn) is with Shenyang aerospace University; Shenyang, 110136, China;*
- *Mohammed A.(alqaness@whu.edu.cn) is with State Key Laboratory for Information Engineering in Surveying, Mapping, and Remote Sensing, Wuhan University, Wuhan 430079, China;*
- *Xingfu Wang and Liang Zhao are the corresponding authors.*

quantities do not thoroughly actualize the main parameters that influence network's layer in VANETs. The performance of VANET is mostly evaluated through three essential metrics, namely end-to-end latency, delivery ratio, and communication overhead. These metrics are interrelated with multiple criteria. Latency is proportionally correlated to the distance between the source and destination. Longer distance leads in general to more hops, more junctions from source to destination, and more carry-and-forward times. This definitely results in more network's partitions and upsurges the latency. Despite it is desirable for the data packet to travel through shorter-distance segments, the shortest-distance segments are not always an efficient selection because the connectivity of such segments is not constantly guaranteed. Higher density inevitably improves network connectivity and reduces the number of carry-and-forwards, thereby reducing latency. Moreover, higher density allows packets to travel primarily on selected segments, thus reducing switching failures of packets at junctions and reducing the latency as well. Likewise, a longer distance decreases the delivery ratio because packets may encounter network's partitions, which is considered as the main reason for packets dropping. Longer distance also has an impact on communication overhead because it is necessary to select more forwarders through multi-hops, and then more operations need to be coordinated all the way. Furthermore, the process of packet switching is increased with longer distance, which in turn increases the overhead, especially when the packet fails to be switched. Vehicle's speed, movement direction, and other quantities such as signals fading and communication range had an impact on network performance. These quantities entirely captured the performance of VANETs, and are deeply explained and mathematically modeled in Section 4. This motivated us to design *Heuristic Routing for Vehicular Networks* (HERO), which considers seven quantities to select the next-hop segment (*inter-routing*) and four quantities to select the next-hop vehicle (*intra-routing*).

Contributions: We developed a routing protocol, namely HERO, which operates in a distributed manner to heuristically select the road segments and the relay vehicles. The selection of road segments is based on two heuristic functions. The first heuristic function aims to select the *Shortest Distance* by aggregating three quantities, dot production angle, perpendicular distance, and segment length. The second heuristic function considers the segment connectivity through four quantities, range of communication, lanes count, segment length, and the mean vehicle count. On the other hand, the selection of relay vehicles is attained by considering four quantities, the moving direction of the vehicle, speed difference, signal fading, and buffer size. Simulation and documentation of HERO are available online in the link[1].

Organization: The rest of this paper is organized as follows. Section 2 explains previous studies. Section 3 explains the preliminaries, including the traffic and propagation models. Section 4 explains the proposed protocol, while the performance analysis is elaborated in Section 5. The experiments and discussions are explained in Section 6. Finally, Section 7 concludes this work.

2. RELATED WORK

From the perspective of network structure, the routing protocols are classified into clustered-structure and flat-structure. MOZO (***Mo****ving* ***Zo****ne*) [14] is an example of clustered-based, which partitioned the road network to disjoint zones according to the similarity of movement, which is actually computed through considering multiple criteria such speed, time stamp, and the direction of movement. Each zone has a header vehicle that manages the member vehicles in the zone as well as dissimilates the data packets. BRAVE is an example of flat-structure, introduced in [16], it employed an opportunistic scheme, in which the relay vehicles are selected based on the shortest distance. BRAVE operates in two main steps, opportunistic data forwarding, and spatial awareness. In spatial awareness, BRAVE selects the road segment by employing Dijkstra's algorithm, in which network information and digital map-street are utilized. In the second step, the packets are opportunistically routed on the selected road segment.

Furthermore, from the perspective of network infrastructures, the routing protocols in VANET are classified into pure *vehicle-to-vehicle* routing (V2V) and *vehicle-to-vehicle* assisted by *roadside units* routing (V2I). Due to the slow deployment of *roadside units*, most of the studies consider V2V routing strategy e.g., [12], [14], [16], [17], and [18]. However, recently a few studies have considered the V2I e.g., [5], [15], [19], [20], and [21]. An example of V2V is DEEP (*Density-aware Emergency Message Extension Protocol*) [18]. DEEP divides roads into multiple equal-sized blocks based on vehicle density and assigns different priorities to vehicles. Each block is assumed to contain one vehicle. The farther block has a shorter delay time than the closer block to forward the emergency messages. Low density results in larger block sizes, and as the density becomes higher, the block size becomes smaller. On the other hand, an example of V2I is *Hidden Markov Model* (PRHMM) [15]. PRHMM supports V2V and V2I; it predicts the upcoming vehicle's location based on its historical mobility patterns and predicts the movement pattern toward the destination using *Hidden Markov Model*. The vehicle that has a higher probability of reaching the destination is selected as a next-hop in the path.

Map-based protocols utilize GPS and digital maps to select the routing path between the source and the destination. Examples of *Map-based* routing are addressed in [17] and [12]. In [17], a street-centric routing protocol, called SRPMT (*Street-Centric Routing Protocol based on Micro-topology*), was proposed. SRPMT is designed based on the concept of *Micro-topology* (i.e., the road segment between two consecutive intersections), which considers the mobility of the vehicle, the signal fading, the wireless channel contention, and existing data traffic. SRPMT runs in two steps, the selection of the next successive road segments based on *Dijkstra's algorithm* and the packet routing within the road segment based on an opportunistic metric that considers

[1] https://github.com/howbani/VSIM

the end-to-end delay. An opportunistic metric ETCoP (expected transmission cost over a multi-hop path) is proposed in [12]. ETCoP is based on *link correlation,* which mathematically expresses how the transmission cost of a given packet is influenced when distinct links are utilized. Based on ETCoP, the authors designed SRPE (street-centric opportunistic routing protocol), which runs in two steps as in SRPMT.

Adaptive multiple-hop routing protocols are proposed in [22] and [23]. Both are designed based on *fuzzy logic,* which is an appropriate computational model, especially for networks with rapid topology variations. PFQ-AODV [22] utilizes fuzzy constraint Q-learning to acquire the routing paths based on AODV routing. Fuzzy logic is employed to evaluate the quality of wireless link through considering multiple criteria such as bandwidth and vehicle movement. In [23], the authors modeled the routing problem as *MCDM,* in which the attributes such as transmission distance, density, and other attributes that have an influence on the network layer are expressed by fuzzy sets, which are embodied by *Fuzzy Membership Functions*. The final decision is derived by using the TSK inference system.

Unlike the previous works, this paper captures multiple quantities when packets are routed. Our work selects road segments with a shorter distance and higher connectivity and prioritizes the vehicles in the selected road segment based on speed difference, the vehicle's moving direction, buffer size, and signal fading.

3. PRELIMINARIES

This section explains the propagation and traffic models used in this article. Notations, which frequently used in this paper, are listed in Table 1.

3.1 Propagation Model

We employed *Nakagami-m propagation model* as formulated in Eq.(1), where $m \geq 1/2$ denotes the path loss while Ω represents the *average power strength* [24] [25]. The CDF of *Nakagami-m* model is formulated as in Eq.(2). The packet is received successfully when the probability of received power is larger than the value r_x as expressed in Eq.(3). Both parameters Ω and r_x are obtained from the *free-space model* as expressed in Eq.(4), where T_p denotes the transmission power, and $d_{i,j}$ denotes the *Euclidian* distance from a sender vehicle n_i to a receiver vehicle n_j. The notations δ, G_t, G_r and λ denote the range of communication, the gain of antenna for the transmitter, the antenna gain for the receiver, and the wavelength of the signal, respectively. Finally, the value of m is derived by Eq. (5) as in [26].

$$f_m(x; m, \Omega) = \frac{m^m . x^{m-1} . e^{-(m/\Omega)x}}{\Omega^m . (m-1)!} \quad (1)$$

$$F_m(x; m, \Omega) = \int_0^x f_m(z; m, \Omega)\, dz = \frac{m^m}{\Omega^m (m-1)!} \int_0^x z^{m-1} e^{-(m/\Omega)z}\, dz \quad (2)$$

$$Pr(x > r_x) = 1 - F_m(r_x; m, \Omega) = e^{-\frac{m}{\Omega} r_x} \sum_{i=0}^{m} \frac{\left(\frac{m}{\Omega} r_x\right)^{i-1}}{(i-1)!} \quad (3)$$

$$\Omega(d_{i,j}) = \frac{T_p}{d_{i,j}^2} G;\ r_x(\delta) = \frac{T_p}{\delta^2}\ ;\ G = \frac{G_t G_r \lambda^2}{16\pi^2} \quad (4)$$

$$m = \begin{cases} 1.0 & d_{i,j} \geq 150m \\ 1.5 & 50m \leq d_{i,j} < 150m \\ 3.0 & d_{i,j} < 50m \end{cases} \quad (5)$$

Table 1: Notations.

Notation	Description
n_i	Vehicle i, located at $(\breve{x}_i, \breve{y}_i)$.
$d_{i,j}$	The distance between the vehicles n_i and n_j.
δ	Denotes the communication range of OBU.
$\mathcal{v}_i, (x_i, y_i)$	$\mathcal{V}_\mathcal{G} = \{\mathcal{v}_0, \mathcal{v}_1, \mathcal{v}_2, \ldots, \mathcal{v}_i\}$ represents road junctions. $\mathcal{v}_s$ denotes the source junction. The destination junction is denoted by $\mathcal{v}_b$. (x_i, y_i) denotes the location of junction $\mathcal{v}_i$.
$\mathcal{r}_{ij}, \lvert\mathcal{r}_{ij}\rvert$	The road segment that joins two junctions $\mathcal{v}_i, \mathcal{v}_j \in \mathcal{V}_\mathcal{G}$. Its length is denoted by $\lvert\mathcal{r}_{ij}\rvert$.
$E_{ij}^R, E_{ij}^S, E_{ij}^T$	E_{ij}^R denotes the expected number of vehicles residing within the segment $\mathcal{r}_{ij}$. E_{ij}^S denotes the average of vehicle speed allowed in the segment $\mathcal{r}_{ij}$. E_{ij}^T denotes the average time that the vehicle resides in $\mathcal{r}_{ij}$.
s_{ij}^{max}	The maximum speed allowed in the segment $\mathcal{r}_{ij}$.
α_{ij}	Interarrival time of vehicles for the segment $\mathcal{r}_{ij}$.
$\theta_{i,j}$	The direction angle between the junctions $\mathcal{v}_i$ and $\mathcal{v}_j$.
$\widetilde{\Phi}_{i,j}$	The distance distribution between the junctions $\mathcal{v}_i$ and $\mathcal{v}_j$.
λ_{ij}	$\lambda_{ij} = 1/\alpha_{ij}$ is the arrival rate of vehicles to the segment $\mathcal{r}_{ij}$.
$\widetilde{\wp}_{ij}, \tilde{Q}_{i,j}$	The heuristic function of *Inter-Path* and the heuristic function of *Intra-Path*, respectively.
$\tilde{\psi}_{i,j}, \tilde{\mathcal{L}}_{i,j}$	The perpendicular distance distribution and road segment length distribution, respectively.
$\tilde{\mathcal{S}}_{i,j}, \widetilde{\mathcal{D}}_{i,j},$ $\widetilde{\mathcal{M}}_{i,j}, \tilde{\mathcal{F}}_{i,j}$	Speed difference distribution, moving direction distribution, buffer size distribution and signal fading distribution, respectively.
$\bar{\chi}_{i,j}$	Mobility similarity score.

3.2 Road Network and Traffic Model

The road network that contains $\lvert\mathcal{V}_\mathcal{G}\rvert$ junctions or intersections and $\lvert\mathcal{E}_\mathcal{G}\rvert$ road segments can be modeled by a directed graph $\mathcal{G} = (\mathcal{V}_\mathcal{G}, \mathcal{E}_\mathcal{G})$, such that the junctions represent the vertices set $\mathcal{V}_\mathcal{G} = \{\mathcal{v}_0, \mathcal{v}_1, \mathcal{v}_2, \ldots, \mathcal{v}_i\}$, while the road segments (multi-lanes as shown in Fig.1) represent the edges set $\mathcal{E} \subseteq \mathcal{V}_\mathcal{G} \times \mathcal{V}_\mathcal{G}$. Let $\mathcal{r}_{i,j}$ be the road segment that joins the junctions $\mathcal{v}_i, \mathcal{v}_j \in \mathcal{V}_\mathcal{G}$. For a given road segment $\mathcal{r}_{i,j}$, the *interarrival time* (in seconds) of two successive arrivals is modeled by *exponential distribution* with the parameter $\alpha_{i,j} > 0$. This means that any arrival occurs at any given time is independent of the length of time that has elapsed from the previous arrival [27], [5]. The PDF of the *exponential distribution* is formulated by Eq. (6). For a given road network $\mathcal{G} = (\mathcal{V}_\mathcal{G}, \mathcal{E}_\mathcal{G})$with $\lvert\mathcal{E}_\mathcal{G}\rvert$ segments, each segment $\mathcal{r}_{i,j}$ has different *interarrival mean* $\alpha_{i,j}$ due to some factors such as the time or the location of the segment in the city. At the simulation level, the mean value of $\alpha_{i,j}$ is obtained by *Box–Muller Transform* Eq. (7), where μ_I and σ_I denote *mean* and the *deviation* of *Gaussian* distribution, respectively.

$$I_{i,j}(t, \alpha_{i,j}) = \alpha_{ij} e^{-t\alpha_{i,j}} \quad (6)$$

$$\alpha_{i,j} = \left|\mu_I + \left(\sigma_I \sqrt{-2\, log\, z_0}\ sin(2\pi z_1)\right)\right|;\ z_0, z_1 \in [0,1];\ \forall \mathcal{r}_{i,j} \in \mathcal{E}_\mathcal{G} \quad (7)$$

For a given road segment, the arrival of vehicles follows Poisson process with a rate $\lambda_{i,j} = 1/\alpha_{i,j}$. Thus, the probability that k vehicles arrive at the entry of $\mathcal{r}_{ij}$ in one second is obtained by the *probability mass function* Eq. (8).

$$A_{i,j}(k) = \frac{\lambda_{i,j}^k}{k!} e^{-\lambda_{i,j}} \quad (8)$$

The probability that k vehicles reside within $r_{i,j}$ is given by the mass function Eq. (9), where $|r_{i,j}|$ denotes the segment length, and $\rho_{i,j} = \lambda_{i,j}|r_{i,j}|$ is the density of the road segment $r_{i,j}$ (vehicles per segment) [5]. $E^S_{i,j}$ is the average speed of vehicles allowed in the segment $r_{i,j}$, formulated by Eq.(10) where $\bar{l}$ is the average length of a vehicle, and s^{max}_{ij} is the maximum speed allowed in the segment $r_{i,j}$. $E^R_{i,j}$ denotes the expected number of vehicles residing within the segment $r_{i,j}$ which is obtained from Little's Law Eq. (11) where $E^T_{i,j} = |r_{i,j}|/E^S_{i,j}$ is the average time that the vehicle resides in $r_{i,j}$.

$$R_{i,j}(k) = \frac{(\rho_{i,j})^k}{k!}\, e^{-\rho_{i,j}} \tag{9}$$

$$E^S_{i,j} = s^{max}_{i,j}\left(1 - \frac{\bar{l}\, E^R_{i,j}}{|r_{i,j}|}\right) \tag{10}$$

$$E^R_{i,j} = \lambda_{i,j}\, E^T_{i,j} \approx \sum_{x=0}^{|r_{i,j}|/\bar{l}} x.R_{i,j}(x) \tag{11}$$

At the simulation level, for a given segment $r_{i,j} \in \mathcal{E}_{\mathcal{G}}$, the maximum speed $s^{max}_{i,j}$ is obtained by *Box–Muller Transform* Eq. (12), where μ_S and σ_S are the *mean* and the *deviation* of *Gaussian* distribution, respectively.

$$s^{max}_{i,j} = \left|\mu_S + \left(\sigma_S\sqrt{-2\log z_0}\, \sin(2\pi z_1)\right)\right|; z_0, z_1 \in [0,1];\ \forall r_{ij} \in \mathcal{E}_{\mathcal{G}} \tag{12}$$

The per-vehicle speed is modeled by a random variable that follows *truncated normal distribution* with density function Eq. (13).

$$S_{i,j}(s_k) = \frac{1}{\sigma_S\sqrt{2\pi}} e^{\left(\frac{s_k - E^S_{i,j}}{\sigma_S\sqrt{2}}\right)^2} \Bigg/ \int_{s^{min}_{i,j}}^{s^{max}_{i,j}} \frac{1}{\sigma_S\sqrt{2\pi}} e^{\left(\frac{s_k - E^S_{i,j}}{\sigma_S\sqrt{2}}\right)^2} \tag{13}$$

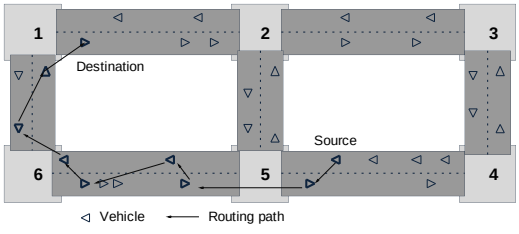

Fig.1: Road network.

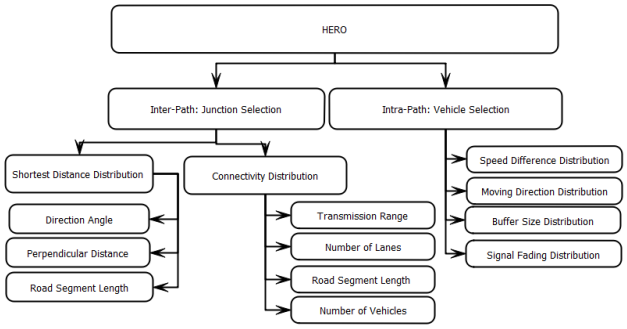

Fig.2: The main components of HERO.

4. THE PROPOSED PROTOCOL

For a given junction $v_i \in \mathcal{V}_{\mathcal{G}}$, let $\mathcal{V}_i = \{v_j | v_j \in \mathcal{V}_{\mathcal{G}}\ \&\ r_{i,j} \in \mathcal{E}_{\mathcal{G}}\}$ be the set of adjacent junctions of v_i. For example, in Fig.1, $\mathcal{V}_2 = \{v_1, v_3, v_5\}$. The position of v_i is denoted by (x_i, y_i). The source junction is denoted by v_s while the destination junction is denoted by v_b.

To achieve the three goals of this work, we propose a solution that subdivided the problem into two main components; each is characterized by a heuristic function as depicted in Fig.2. The two heuristic functions, *Inter-path* and *Intra-path* are proposed to improve the selection of road segments and relay vehicles, respectively. *Inter-path* is designed to select a routing path that consists of multiple road segments with a shorter distance and higher connectivity. This is implemented through two probability distributions, *Shortest Distance Distribution* (SDD) and the *Connectivity Distribution* (CD). SDD considers three quantities, direction angle, perpendicular distance, and segment length, while CD considers four quantities, communication range, lanes count, length of segment, and the expected vehicles count. On the other hand, *Intra-path* prioritizes the relay vehicles based on four quantities, speed difference, vehicle's moving direction, buffer size, and signal fading. All these quantities are explained thoroughly in the following subsections. An illustrative numerical example for *Intra-Path* and *Inter-Path* are involved in the supplementary file[2].

4.1 Inter-Path: Junction Selection

An *Inter-path* is a sequence of consecutive junctions connecting the source to the destination junctions, heuristically satisfying two key requirements, shorter routing-distance and higher connectivity. The selection decision is aggregated through weighted averaging $\tilde{\wp}_{i,j}$ Eq.(14) with two probability distributions, connectivity distribution (denoted by $\tilde{\xi}_{i,j}$ Eq.(26)) and the shortest distance distribution (denoted by $\tilde{\Phi}_{i,j}$ Eq.(15)). The priority of the selection (i.e., for the junction $v_i \in \mathcal{V}_{\mathcal{G}}$) is computed in a distributed manner as expressed in Eq.(14) where w_Φ and w_ξ are tuning parameters.

$$\tilde{\wp}_{i,j} = w_\Phi \tilde{\Phi}_{i,j} + w_\xi \tilde{\xi}_{i,j} \Big/ \sum_{\forall v_x \in \mathcal{V}_i} w_\Phi.\tilde{\Phi}_{i,x} + w_\xi \tilde{\xi}_{i,x}\ \ \forall v_j \in \mathcal{V}_i;\ \ w_\Phi + w_\xi = 1; \tag{14}$$

ALGORITHM 1 outlines the selection of the next segment, given that a vehicle is heading toward a junction v_i.

ALGORITHM 1: Road Segment Selection.
Input: Current junction v_i; destination junction v_b.
Output: The road segment r_{ij} with the highest priority.

```
1.  JunctionSelection( v_i, v_b)
2.  {
3.    ∀ v_j ∈ V_i  Do
4.      {
5.        Compute θ̃_{i,j} by Eq.(17). // Dot angle production.
6.        Compute ψ̃_{i,j} by Eq.(20). // Perpendicular distance.
7.        Compute L̃_{i,j} by Eq.(22). // Segment length.
8.        Compute Φ̃_{i,j} by Eq.(15).// Shortest Distance Distribution.
9.        Compute ξ̃_{i,j} by Eq.(26).//  Connectivity Distribution.
10.     }
11.   ∀ v_j ∈ V_i  Do
12.       Compute ℘̃_{ij} by Eq.(14).// Segment priority.
13.    return r_{ij}  with the max ℘̃_{ij}.
14. }
```

4.1.1 Shortest Distance Distribution (SDD)

[2] https://github.com/howbani/VSIM/blob/master/suppl.pdf

The *shortest distance distribution* $\tilde{\Phi}_{i,j}$ is obtained by combining three *probability mass functions*, formularized in Eq. (15), including the *direction angle* $\theta_{i,j}$, the *perpendicular distance* $\tilde{\psi}_{i,j}$ and the segment's length $\tilde{\mathcal{L}}_{i,j}$. The direction distribution assigns higher priority for junctions that are toward the destination junction, while the perpendicular distance distribution assigns higher priority for junctions that are closer to the centerline between the source and the destination (see Fig. 3). The shortest distance is computed by summing the perpendicular distance and segment length, all multiplied by the direction. This ensures that as long as the direction is correct, both the perpendicular distance and segment length will have an impact. Obviously, the direction has the greatest impact, while both perpendicular distance and segment length have an equal impact.

$$\tilde{\Phi}_{i,j} = \tilde{\theta}_{i,j}(\tilde{\psi}_{i,j} + \tilde{\mathcal{L}}_{i,j}) \Big/ \sum_{\forall \nu_x \in \mathcal{V}_i} \tilde{\theta}_{i,x}(\tilde{\psi}_{i,x} + \tilde{\mathcal{L}}_{i,x}) \quad \forall \nu_j \in \mathcal{V}_i; \tag{15}$$

Direction Angle. The *direction angle* $\theta_{i,j}$ between the current junction ν_i and the potential next-junction ν_j towards the destination junction ν_b is modeled as a dot product of two vectors $\vec{a}.\vec{c}$, such that $\vec{a} = (x_j - x_i, y_j - y_i)$ and $\vec{c} = (x_b - x_i, y_b - y_i)$, and normalized to π by Eq. (16). The normalized-direction $\bar{\theta}_i = (\bar{\theta}_{i,1}, \bar{\theta}_{i,2}, \dots, \bar{\theta}_{i,b_i})$ is injected into the mass function Eq. (17) to obtain the random variable $\tilde{\theta}_i = (\tilde{\theta}_{i,1}, \tilde{\theta}_{i,2}, \dots, \tilde{\theta}_{i,b_i})$. Direction distribution assigns a higher probability for the normalized angles $0 \le \bar{\theta}_{i,j} \le \frac{1}{2}$ that ensure higher routing progress toward the destination junction.

$$\bar{\theta}_{i,j} = cos^{-1}\left(\frac{(x_j - x_i)(x_b - x_i) + (y_j - y_i)(y_b - y_i)}{\sqrt{(x_b - x_i)^2 + (y_b - y_i)^2}\sqrt{(x_j - x_i)^2 + (y_j - y_i)^2}} \right) / \pi \tag{16}$$

$$\tilde{\theta}_{i,j} = \begin{cases} \left(1 - \frac{\bar{\theta}_{i,j} e^{\bar{\theta}_{i,j}}}{1 + \bar{\theta}_{i,j} e^{\bar{\theta}_{i,j}}}\right)^{\tau} \Big/ \sum_{\forall \nu_x \in \mathcal{V}_i} \left(1 - \frac{\bar{\theta}_{i,x} e^{\bar{\theta}_{i,x}}}{1 + \bar{\theta}_{i,x} e^{\bar{\theta}_{i,x}}}\right)^{\tau} \\ \tau = 1; \frac{1}{2} \ge \bar{\theta}_{i,j} \ge 0 \\ \tau = 2; \frac{1}{2} \le \bar{\theta}_{i,j} \le 1 \end{cases} \quad \forall \nu_j \in \mathcal{V}_i; \tag{17}$$

Perpendicular Distance. *Perpendicular distance* distribution $\tilde{\psi}_{i,j}$ allocates higher probability for the junctions that are closer to the central line $l_{s,b}$ (i.e., a virtual line linking the source junction ν_s and the destination junction ν_b, see Fig.3, Assume that ν_4 is the current junction, $\mathcal{V}_4 = \{\nu_s, \nu_2, \nu_3, \nu_5, \nu_6, \nu_7\}$. The two heads arrow indicates the central line $l_{s,b}$ and dash lines indicate the *Perpendicular distance* for junctions in $\mathcal{V}_4$). The perpendicular distance ψ_j from ν_j to $l_{s,b}$ is defined by Eq.(18). For the source junction ν_i, we define the normalized perpendicular-distance random variable $\bar{\psi}_i = (\bar{\psi}_{i,1}, \bar{\psi}_{i,2}, \dots, \bar{\psi}_{i,b_i})$ by Eq. (19). Furthermore, we define the perpendicular-distance probability distribution, denoted by $\tilde{\psi}_i = (\tilde{\psi}_{i,1}, \tilde{\psi}_{i,2}, \dots, \tilde{\psi}_{i,b_i})$, by Eq. (20).

$$\psi_j = \frac{|x_j(y_b - y_s) - y_j(x_b - x_s) + x_b y_s - y_b x_s|}{\sqrt{(x_b - x_s)^2 + (y_b - y_s)^2}} \tag{18}$$

$$\bar{\psi}_{i,j} = \frac{\psi_j}{\sum_{\forall \nu_x \in \mathcal{V}_i} \psi_x} \forall \nu_j \in \mathcal{V}_i; \tag{19}$$

$$\tilde{\psi}_{i,j} = e^{-\bar{\psi}_{i,j}} \Big/ \sum_{\forall \nu_x \in \mathcal{V}_i} e^{-\bar{\psi}_{i,x}} \quad \forall \nu_j \in \mathcal{V}_i; \tag{20}$$

Road Segment Length. This distribution allocates a higher probability to the longer segment. This is because longer segments are preferable to avoid frequent segment switching that leads to hinder packet delivery, especially when the vehicle density increases. For the source junction ν_i, we define the normalized segment length random variable $\bar{\mathcal{L}}_i = (\bar{\mathcal{L}}_{i,1}, \bar{\mathcal{L}}_{i,2}, \dots, \bar{\mathcal{L}}_{i,b_i})$ by Eq. (21). Furthermore, we define the segment length probability distribution, denoted by $\tilde{\mathcal{L}}_i = (\tilde{\mathcal{L}}_{i,1}, \tilde{\mathcal{L}}_{i,2}, \dots, \tilde{\mathcal{L}}_{i,b_i})$, by the mass function as formulated in Eq. (22).

$$\bar{\mathcal{L}}_{i,j} = \sqrt{(x_j - x_i)^2 + (y_j - y_i)^2} \Big/ \sum_{\forall \nu_k \in \mathcal{V}_i} \sqrt{(x_k - x_i)^2 + (y_k - y_i)^2} \, \forall \nu_j \in \mathcal{V}_i; \tag{21}$$

$$\tilde{\mathcal{L}}_{i,j} = \left(1 - \sqrt{e^{-\bar{\mathcal{L}}_{i,j}}}\right) \Big/ \sum_{\forall \nu_x \in \mathcal{V}_i} \left(1 - \sqrt{e^{-\bar{\mathcal{L}}_{i,x}}}\right) \quad \forall \nu_j \in \mathcal{V}_i; \tag{22}$$

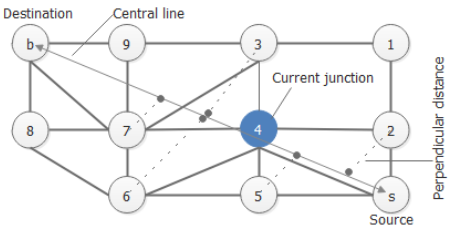

Fig.3: Perpendicular distance.

4.1.2 Connectivity Distribution (CD)

The connectivity of a given road segment $r_{i,j} \in \mathcal{E}_g$ is entirely hinged on the density of vehicles and the *inter-distance* of vehicles. Hence, the density is computed based on multiple parameters such as communication range δ, expected number of vehicles, the road segment length, and lanes count. We defined the special density of vehicles by Eq.(23), where γ represents the lanes count on the road segment, and $E^R_{i,j}$ denotes the expected number of vehicles on $r_{i,j}$, obtained by Eq.(11).

$$\rho_{i,j} \triangleq \frac{\delta.\gamma.E^R_{i,j}}{|r_{i,j}|}; \tag{23}$$

To compute the segment connectivity, the road segment is divided into $2|r_{i,j}|/\delta$ equal blocks such that each block's length is $\delta/2$ meters. Thus, we obtained the probability of having k vehicle(s) on a block by *Poisson* distribution, as expressed by Eq.(24). A block is connected if it holds at least one vehicle; this is obtained by Eq.(25). Thus, a road segment is connected, providing that its blocks are connected, as derived by Eq.(26).

$$\hat{R}_{i,j}(k) = \frac{(\rho_{i,j})^k}{k!} e^{-\rho_{i,j}} \; ; \tag{24}$$

$$\hat{R}_{i,j}(k > 0) = 1 - \hat{R}_{i,j}(0) = 1 - e^{-\rho_{i,j}} \; ; \tag{25}$$

$$\xi_{i,j} = \prod_{c=1}^{2|r_{i,j}|/\delta} \left(1 - e^{-\rho_{i,j}}\right) = \left(1 - e^{-\rho_{i,j}}\right)^{\frac{2|r_{i,j}|}{\delta}} \; ; \tag{26}$$

Eq. (26) expresses the relationships among the five parameters, which are the segment connectivity, range of communication, lanes count, segment length, and the expected vehicles count on a given road segment. To evaluate the performance of Eq. (26), we selected the following default settings. The number of vehicles is set to 5, segment length is set to 1000m, transmission range is set to 100m, and the number of lanes for each roadway is set to 3. Three

evaluation scenarios are considered. In the first scenario, both the segment length and the number of vehicles are varied. The number of vehicles varies from 1 to 20, and the length of the road segment is varied from 300m to 3000m. The evaluation results are shown in Fig.4 and Fig.5. Fig.4 shows that for a given segment length, the segment connectivity gets higher as the number of vehicles increases. While Fig.5 shows that for a given number of vehicles, the connectivity gets lower as the segment length increases. In the second scenario, both the transmission range and the number of vehicles are varied. The evaluation results are shown in Fig.6. It shows that for a given transmission range, the segment connectivity gets higher as the number of vehicles increases.

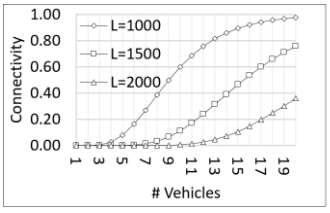

Fig.4: Road segment connectivity varying road segment length and vehicles count.

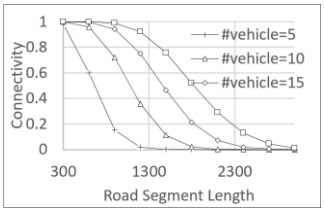

Fig.5: Road segment connectivity varying the length of road segment and the vehicles count.

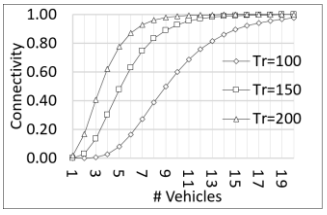

Fig.6: Road segment connectivity. Varying transmission range and the number of vehicles.

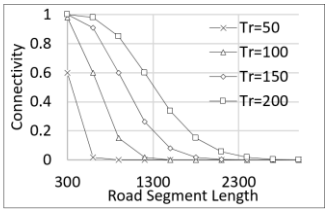

Fig.7: Road segment connectivity. Varying transmission range and road segment length.

In the third scenario, both the transmission range and the road segment length are varied. The evaluation results are shown in Fig.7. It shows that for a given transmission range, the connectivity gets higher as the segment length decreases. Like [28], during simulations, we considered different transmission ranges 100m, 250m, and 1000m for different devices.

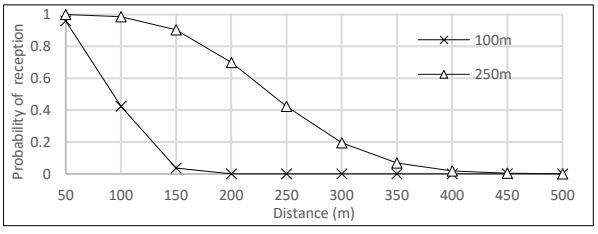

Fig.8: The probability of receiving the packet over a given distance. Two values of transmission ranges are utilized 100m and 250m.

4.2 Intra-Path: Vehicle Selection

Intra-Path selects the relay vehicles in a distributed manner. Thus, a vehicle n_i should know its neighbors, denoted by $\mathbb{N}_i$, via broadcasting beacon packet. To maintain its neighbor set, vehicle n_i periodically broadcasts beacon packets [5]. When it has a data packet to send, n_i selects a candidate set, denoted by $\mathbb{C}_i \subseteq \mathbb{N}_i$, which is computed according to a specific routing metric [29][30]. From the candidate set $\mathbb{C}_i$, the sender vehicle selects one forwarder vehicle ($n_j \in \mathbb{C}_i$) to relay the packet. The process of selecting one forwarder from the candidate set is called the *candidate coordination*. This section presents a new routing metric that enhances the delivery ratio and reduces delivery delay in urban environments. We define our routing metric for each node n_i as a random variable $\tilde{\mathcal{Q}}_i = \{\tilde{\mathcal{Q}}_{i,1}, \tilde{\mathcal{Q}}_{i,2}, \dots, \tilde{\mathcal{Q}}_{i,q_i}\}$ by the mass function Eq.(27), which combines four probability distributions, the speed difference $\tilde{\mathcal{S}}_{i,j}$(Eq.(28)), the direction $\tilde{\mathcal{D}}_{i,j}$ (Eq.(29)), the available buffer size $\tilde{\mathcal{M}}_{i,j}$ (Eq.(30)) and the signal fading $\tilde{\mathcal{F}}_{i,j}$(Eq.(32)). Considering the jointly effect on Eq. (27), the moving direction has the greatest effect, while the other three distributions $\tilde{\mathcal{S}}_{i,j} + \tilde{\mathcal{F}}_{i,j} + \tilde{\mathcal{M}}_{i,j}$ have an equal effect. ALGORITHM 2 outlines the selection of the next vehicle.

ALGORITHM 2: Vehicle Selection.
Input: Sender vehicle n_i; destination vehicle n_b.
Output: The next vehicle forwarder n_j with the highest priority.

```
1.  VehicleSelection( n_i, n_b)
2.  {
3.    ∀ n_j ∈ N_i  Do
4.      {
5.        Compute S̃_{i,j} by Eq.(28). // Speed Difference.
6.        Compute D̃_{i,j} by Eq.(29). // Moving Direction.
7.        Compute M̃_{i,j} by Eq.( 30). // Buffer Size Distribution.
8.        Compute F̃_{i,j} by Eq.(32).// Signal Fading Distribution.
9.        Compute   D̃_{i,j}(S̃_{i,j} + F̃_{i,j} + M̃_{i,j}).
10.     }
11.   ∀ n_j ∈ N_i  Do
12.       Compute Q̃_{i,j} by Eq.(27).// Vehicle priority.
13.   return vehicle n_j with the max Q̃_{i,j}.
14. }
```

$$\tilde{\mathcal{Q}}_{i,j} = \frac{\tilde{\mathcal{D}}_{i,j}\left(\tilde{\mathcal{S}}_{i,j} + \tilde{\mathcal{F}}_{i,j} + \tilde{\mathcal{M}}_{i,j}\right)}{\sum_{\forall n_x \in \mathbb{N}_i} \tilde{\mathcal{D}}_{i,x}\left(\tilde{\mathcal{S}}_{i,x} + \tilde{\mathcal{F}}_{i,x} + \tilde{\mathcal{M}}_{i,x}\right)} \; \forall\, n_j \in \mathbb{N}_i \qquad (27)$$

4.2.1 Speed Difference Distribution

Network performance can be enhanced by considering the least speed difference between two moving vehicles as both stay longer together and nearer to one another, which decreases the broadcasting of beacons between them. We will explain this later in the *Neighbors Assortment* (ALGORITHM 4). *Speed Difference Distribution* considers the similarity of speed between the moving vehicles such that greater priority-values are allocated to those with the least difference of speed. The speed difference is modeled as a random variable such that the sender vehicle n_i has a speed difference random variable $\tilde{\mathcal{S}}_i = \{\tilde{\mathcal{S}}_{i,1}, \tilde{\mathcal{S}}_{i,2}, \dots, \tilde{\mathcal{S}}_{i,q_i}\}$ given by the mass function Eq.(28) where s_i denotes the current speed of the vehicle n_i.

$$\tilde{\mathcal{S}}_{i,j} = e^{-\left(\frac{\sqrt{(s_i - s_j)^2}}{max(s)}\right)} \Bigg/ \sum_{\forall n_x \in \mathbb{N}_i} e^{-\left(\frac{\sqrt{(s_i - s_x)^2}}{max(s)}\right)} \; \forall\, n_j \in \mathbb{N}_i \qquad (28)$$

4.2.2 Moving Direction

We assume that the vehicle n_i located at $(\check{x}_i, \check{y}_i)$ is currently on the road segment r_{sd} that connects the start junction v_s and the end junction v_d. Vehicle n_i should select one relay vehicle $n_j \in \mathbb{N}_i$ which is currently in front of n_i. Vehicles in

front of n_i are determined by the angle β between two vectors as formulated in Eq.(29). In the case of the network partition, to take advantage of the vehicles which are not in the same direction as the current sender, HERO allows the sender vehicle to select the next-forwarder from the opposite direction. This is implemented through the parameters Δ (same direction) and ∇ (opposite direction) as in Eq.(29). The smaller value of Δ allocates greater priority for the vehicles that are in the same direction as the sender. Likewise, a greater value of ∇ assigns a smaller priority for the vehicles which are in opposite directions.

$$\beta = cos^{-1}\left(\frac{(\check{x}_j - \check{x}_i)(x_d - \check{x}_i) + (\check{y}_j - \check{y}_i)(y_d - \check{y}_i)}{\sqrt{(x_d - \check{x}_i)^2 + (y_d - \check{y}_i)^2}\sqrt{(\check{x}_j - \check{x}_i)^2 + (\check{y}_j - \check{y}_i)^2}}\right)/\pi$$

$$\widetilde{\mathcal{D}}_{i,j} = \begin{cases} \left(1 - \frac{\beta e^{\beta}}{1+\beta e^{\beta}}\right)^{\Delta}; 0 < \Delta \leq 1; \quad \beta \leq \frac{1}{2}; \\ \left(1 - \frac{\beta e^{\beta}}{1+\beta e^{\beta}}\right)^{\nabla}; \ 1 < \nabla \leq 5; \beta \geq \frac{1}{2}; \end{cases} \quad \forall\, n_j \in \mathbb{N}_i \qquad (29)$$

4.2.3 Buffer Size Distribution

In order to reduce the queuing delay, that is, the time a packet waits in the queue until it can be relayed, this distribution assigns higher priority for the vehicle with more available buffer (i.e., fewer packets in the queue). Let $\acute{m}$ be the buffer size and let $m_j \leq \acute{m}$ be the current number of packets in the buffer of vehicle n_j. The sender vehicle defines a random variable $\widetilde{\mathcal{M}}_i = \{\widetilde{\mathcal{M}}_{i,1}, \widetilde{\mathcal{M}}_{i,2}, \dots, \widetilde{\mathcal{M}}_{i,q_i}\}$ by the mass function Eq.(30).

$$\widetilde{\mathcal{M}}_{i,j} = \frac{e^{-\frac{m_j}{\acute{m}}}}{1 + \frac{m_j}{\acute{m}}} = \frac{\acute{m}.e^{-\frac{m_j}{\acute{m}}}}{\acute{m} + m_j} \quad \forall\, n_j \in \mathbb{N}_i \qquad (30)$$

4.2.4 Signal Fading Distribution

Signal fading is modeled as *Nakagami distribution* with $m = 3$ as shown in Eq.(31)[25]. By applying $\Omega(d_{i,j})$ and $r_x(\delta)$ of Eq.(4) to Eq.(31), the probability of receiving the packet over the transmission distance $d_{i,j}$ is obtained by Eq.(32) where $d_{i,j}$ is the distance between the sender vehicle n_i and the receiver n_j, see Fig.8. For a given sender vehicle n_i, signal fading to its neighboring vehicles is modeled as a random variable $\tilde{\mathcal{F}}_i = \{\tilde{\mathcal{F}}_{i,1}, \tilde{\mathcal{F}}_{i,2}, \dots, \tilde{\mathcal{F}}_{i,q_i}\}$. Note that signal fading is a function of transmission distance and communication range. The transmission distance is obtained from the received signal strength indicator as in [31].

$$Pr(x > r_x) = e^{-\frac{3}{\Omega}r_x} \sum_{i=0}^{3} \frac{\left(\frac{m}{\Omega} r_x\right)^{i-1}}{(i-1)!} = e^{-3\left(\frac{r_x}{\Omega}\right)}\left(1 + 3\left(\frac{r_x}{\Omega}\right) + 4.5\left(\frac{r_x}{\Omega}\right)^2\right) \qquad (31)$$

$$\tilde{\mathcal{F}}_{i,j} = e^{-3\left(\frac{d_{i,j}}{\delta}\right)^2}\left(1 + 3\left(\frac{d_{i,j}}{\delta}\right)^2 + 4.5\left(\frac{d_{i,j}}{\delta}\right)^4\right) \qquad (32)$$

4.3 Neighbors Assortment and Data Routing

Data packets are routed from a source to a destination according to the procedures outlined in ALGORITHM 3. Given a sender vehicle n_k which is currently traveling on the road segment $r_{ij} = (v_i, v_j)$. Let $\mathcal{H}(n_k, v_j)$ be the heading distance to the junction v_j (i.e., the remaining distance until the vehicle n_k reaches the end junction v_j). We define $\widehat{\mathcal{H}} = \delta/2$ as the heading distance threshold. If $\mathcal{H}(n_k, v_j)$ is smaller than the threshold $\widehat{\mathcal{H}}$, the vehicle n_k starts selecting a new road segment r_{jx} by ALGORITHM 1. After selecting the road segment r_{jx}, the vehicle n_k searches for its neighbors in r_{jx} by sending beacon packet and prioritizes the neighboring vehicles by ALGORITHM 2. On the other hand, as long as the heading distance is greater than the threshold, the vehicle picks its next-hop from the same road segment.

ALGORITHM 3: Data Routing.
Input: The sender vehicle n_k has a packet in the road segment r_{ij} that joins two intersections v_i, v_j. The destination vehicle n_b.

```
1.  SendPacket(n_k)
2.  {
3.    if H(n_k, v_j) is smaller than Ĥ Do
4.    {
5.      Switch from r_ij to r_jx by JunctionSelection(v_j, v_b), ALGORITHM 1.
6.      Get N_k(r_jx). // the neighbors of n_k in r_jx; the segment r_j,x joins the junctions v_j, v_x.
7.      Select the next vehicle n_v ∈ N_k(r_jx) by VehicleSelection(n_k, n_b), ALGORITHM 2.
8.      if n_v is found Do
9.        ReceivePacket(n_v).
10.     else Do
11.       EnqueuePacket(n_k). n_k stores the packet to be retransmitted later.
12.   }
13.   else // H(n_k, v_j) is greater than Ĥ.
14.   {
15.     Get the neighboring vehicles N_k(r_ij) in the r_ij by sending beacons.
16.     n_v = VehicleSelection(n_k, n_b) in r_ij by ALGORITHM 2.
17.     Goto step line #8.
18.   }
19. } // end SendPacket.
20. ReceivePacket(n_v)
21. {
22.   if n_v is the destination then the routing process is finished.
23.   else SendPacket(n_v).
24. } // end ReceivePacket.
```

ALGORITHM 4: Neighbors Assortment.
Store the neighbor vehicles for a period of time. Assume that n_i receives a packet to be relayed.

```
1.  Assortment (n_i)
2.  {
3.    if N_i is empty Do
4.    {
5.      Send beacon packets.
6.      All OHVs send back a response.
7.      n_i saves all OHVs.
8.      Run ALGORITHM 2 to select the next forwarder.
9.      //save the forwarders with a higher similarity score.
10.     ∀ n_j ∈ N_i Do
11.     {
12.       Compute by χ⃗_i,j by Eq.(33).
13.       if (χ⃗_i,j ≥ 3/4) save n_j in N_i.
14.     }
15.   }
16.   else
17.   {
18.     if keep trace time (KTT) is smaller than the threshold then
19.       Return one candidate from N_k with the highest similarity score.
20.     else clear the N_i;
21.   }
22. }
```

To reduce the overhead and control the number of neighbors, HERO proposes the following algorithm, called *Neighbors Assortment (*ALGORITHM 4*)*, which runs in two steps, initialization and prioritization. In the initialization step, when a sender vehicle n_i has a packet to send, it broadcasts a beacon packet to neighboring vehicles $\mathbb{N}_i$ and waits for one-hop-vehicles (OHVs) to receive that beacon packet and send back a response. In the prioritization step, HERO utilizes the similarity function Eq. (33), which combines the speed difference Eq. (28) and the *Signal Fading* Eq. (32) to prioritize the OHVs according to their similarity score $\vec{\chi}_{i,j}$. The sender stores the ID of vehicles with a higher score $\vec{\chi}_{i,j} \geq 3/4$. The vehicles with higher scores travel longer together and nearer to one another, which means that the sender will use them as fixed neighbors as long as possible. This strategy could reduce the overhead since the sender does not need to broadcast beacons within a period of time (namely the *keep trace-time* (KTT)). The overhead of HERO is analyzed in the next section.

$$\overline{\chi}_{i,j} = e^{-\left(\frac{\sqrt{(s_i-s_j)^2}}{max(s)}\right)-3\left(\frac{d_{i,j}}{\delta}\right)^2}\left(1+3\left(\frac{d_{i,j}}{\delta}\right)^2+4.5\left(\frac{d_{i,j}}{\delta}\right)^4\right) \quad (33)$$

5. Analysis

HERO adopts flat-topology structure [12] [17], that indicates no extra overhead will incur to maintain the clusters (e.g., [32]) or zones (e.g., [14]), especially when vehicles are required to broadcast beacon packets periodically. The flat-topology structure is more efficient regarding overhead, especially for geographical areas with lower vehicle density if the topology changes rapidly. In a flat-topology structure, when the sender vehicle has a data packet, it broadcasts a beacon packet to check the surrounding vehicles. We assumed that each vehicle knows its neighbors or so-called *One-Hop Candidates* (OHC) via broadcasting beacons. A sender vehicle picks a candidate vehicle (i.e., the forwarder) from its candidates to further forward the data packet. To reduce the communication overhead, HERO utilizes the *Neighbors Assortment* (ALGORITHM 4). In HERO, the overhead is computed based on beacon packets count that is required to be exchanged for selecting the next-hop forwarder, which is correlated with the vehicles density and the range of communication. To compute the expected communication overhead, we computed the number of receivers of the beacon packets in each coordination stage (i.e., the selection of the next hope vehicle). This number is calculated by counting the number of OHCs when a sender vehicle transmits a beacon. The probability of having k OHCs within the communication range of the vehicle n_x is derived by Eq.(34), while the expected value of the communication overhead for one-hop is expressed by Eq.(35).

$$\zeta(k) = \frac{(\delta.\lambda)^k}{k!}\, e^{-\delta.\lambda} \quad (34)$$

$$E[C_{hop}] = \sum_{k=0}^{\infty} k.\zeta(k) = e^{-\delta.\lambda}\sum_{k=0}^{\infty} k.\frac{(\delta.\lambda)^k}{k!}$$

$$= \delta.\lambda\,.e^{-\delta.\lambda}\sum_{k=1}^{\infty}\frac{(\delta.\lambda)^{k-1}}{k-1!} = \delta.\lambda\,.e^{-\delta.\lambda}\sum_{j=0}^{\infty}\frac{(\delta.\lambda)^j}{j!}$$

$$= \delta.\lambda\,.e^{-\delta.\lambda}.e^{\delta.\lambda} = \delta.\lambda \quad (35)$$

Furthermore, the communication overhead for a path, $E[C_{path}]$, from a source vehicle to a destination vehicle is derived by Eq. (36), where $E[H]$ denotes the expected hops from a source to a destination, as derived in [33].

$$E[C_{path}] = E[C_{hop}].E[H] \quad (36)$$

The probability mass function that characterizes k hops from a source to a destination is derived by Eq. (37), where $\mathcal{A}$ denotes the *border region*, derived by Eq.(38).

$$\eta(k) = \left(e^{-\lambda\pi\delta^2(k-1)^2} - e^{-\lambda\pi\delta^2k^2}\right)\left(1-e^{\lambda\mathcal{A}/2}\right)^{k-1} \quad (37)$$

$$\mathcal{A} = \delta^2.\left(\frac{\pi-2}{4}\right)+\mathcal{L}.\left(\theta-\frac{sin(2\theta)}{2}\right) \quad (38)$$

The expected hops is obtained by Eq. (39).

$$E[H] = \sum_{k=0}^{\infty} k.\eta(k) = k\sum_{k=0}^{\infty}\left(\left(e^{-\lambda\pi\delta^2(k-1)^2} - e^{-\lambda\pi\delta^2k^2}\right)\left(1-e^{\lambda\mathcal{A}/2}\right)^{k-1}\right) \quad (39)$$

6. Simulation and Evaluation Results

We have conducted extensive simulation experiments to assess the performance of our proposed protocol.

6.1 Environment

We used VSIM [23], which is a 2D simulator provides an acceptable animation and visualization of experimental runs and information about vehicles and road network, available in the link[3].

Table 2: Simulation Parameters.

Parameter	Default value
Network size	4000m×4500m.
Junctions	12 (Traffic light 3s).
Road segments	17 (2000m horizontal, 1500m vertical).
Speed (km/h)	Max. 90 and Min. 0.
Packet size (bytes)	1024 for data 256 for control.
Com. range	500m.
Model	V2V.
Distance	2000m (from the source to the destination).
Storing time	5s (when the network is partitioned).
Retransmission attempts	7 times for RTS, MAC DCF 802.11[2].
# vehicles	400.
Channel data rate	2Mbps.
Radio Propagation	*Nakagami-m*.
Δ, ∇	Δ= 0.1; ∇=3; Eq.(29).
w_Φ, w_ξ	w_Φ = 0.6 and w_ξ = 0.4; Eq.(14).

6.1.1 Settings

The default simulation parameters are listed in Table 2. We used a road network of size 4000m×4500m that contains 12 intersections (with traffic light of 3 seconds) and 17 segments, each segment with two roadways, each of 2 lanes. The starting position of the vehicles is randomly distributed over the road segments. The max allowed speed of the road segment is 90 km/h, while a min speed is 0 km/h. Vehicles gradually decrease the speed when approaching the heading intersection and line-up in a queue to take their turn. The *Inter-Path* is controlled through two turning parameters, w_Φ to control the shortest-distance distribution, while w_ξ is to control the connectivity distribution. Greater value of the turning parameter assigns higher priority for the corresponding distribution. We set the values of tuning parameters w_Φ and w_ξ to 0.6 and 0.4, respectively. The impact of these parameters is enlightened latter in the following subsection. On the other hand, Intra-Path is enhanced through two tuning parameters Δ(same direction) and ∇(opposite direction) to take the advantage of the vehicles which are not in the same direction.

6.1.2 Metrics

- *Communication overhead*: The number of control packets includes beacons, ACK, and the control packets which are intended to maintain the dissemination structure such as cluster or zone.
- *Delivery latency*: The delay time from end-to-end in seconds. It is calculated from the time in which a data packet is generated at the source until it is received by the destination vehicle, including the waiting delay, propagation latency or transmission delay, and queuing latency.
- *Packet success ratio:* The ratio of successfully delivered packets (i.e., to their destinations) to the packets which are generated at the source vehicles.

6.1.3 Comparison Approaches

To meticulously evaluate HERO, we selected two different protocols for comparison, clustering structure and flat structure. The first protocol is a clustered-based protocol

[3] https://github.com/howbani/VSIM

called MOZO [14], while the second protocol is a flat-structure called BRAVE [16]. BRAVE and MOZO are explained in Section 2. MOZO is a new clustering-based protocol and outperformed the existing protocols like CBDRP [32], while BRAVE is selected to represent the non-clustering approaches because BRAVE outperformed SAR, ASTAR, GPCR, and GeOpps, mentioned in [16] and [14]. Due to rapid topology changes, MOZO incurs more communication overhead for building, maintaining, merging, and splitting the zones. Conversely, during data routing, MOZO has lower overhead since member vehicles exclusively communicate with the captain vehicle. One drawback of MOZO is that the road segment is selected by considering the shortest distance without paying attention to the connectivity of the segment, which in some cases makes it possible to drop a packet or slow down its delivery. Different from MOZO, the flat structure BRAVE adopts an opportunistic mechanism to diminish the communication overhead that requires to maintain a hierarchical data dissemination structure.

6.2 Experimental Results

The results reported are the average of 10 independent runs for the same configuration by varying the following parameters, the distance from the source vehicle to destination vehicle, vehicle's number in the road network, the count of packets, and the speed of the vehicles.

6.2.1 Varying Data Packet Delivery Distance

The default number of vehicles is set to 400, while the source vehicles number is set to 100, which are randomly selected at a distance between 600m and 3000m from the destination vehicles, as in [14]. In each simulation run, 100 data packets are generated.

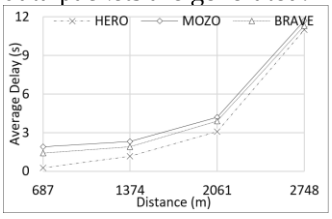

Fig.9: Average delivery latency varying distance.

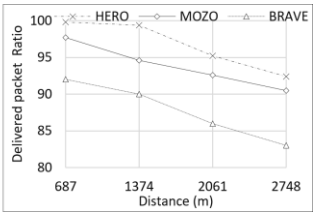

Fig.10: Packet success ratio varying distance.

(a) Delivery Latency. Fig.9 presented the simulation results of delivery latency varying distance values. We concluded that, the longer distance between the source vehicle and destination vehicle undoubtedly leads to more intermediate hops, which increases the latency. The reported results showed that the protocols employed flat-structure (i.e., HERO and BRAVE) outperform the protocols that employed clustered-structure (i.e., MOZO). This is because the flat-structure protocols do not require construction or maintenance. HERO showed faster time than BRAVE and MOZO, owing to the two reasons as follows. Both BRAVE and MOZO employ the shortest path (*Dijkstra's algorithm) to* pick up the next-hop segment without taking into account the segment connectivity Such selection is not always effective because the connectivity of the shortest segment cannot be always guaranteed. In contrast, HERO aggregates both of the segment connectivity and the shortest distance in the heuristic function Eq.(14), which allows HERO to select the road segment professionally. Besides, BRAVE opportunistically selects the next vehicle considering the response time of the ACK without taking into account the speed of the vehicle and the fading of the signal. BRAVE delivers the data packets faster than MOZO, since MOZO's structure needs maintenance and also the complexity of the forwarding mechanism in MOZO which requires relaying the packet of cluster's members to cluster's captain first, and then from the cluster's captain to the next-hop member.

(b) Packet Success Ratio. Fig. 10 presents the simulation results of the packet success ratio varying different distance-values. We concluded that the long distance between the source and destination vehicles gradually decreases the packet success ratio. This primarily due to the reason that the network may subject to partitions with longer distances, which leads to drop the packet. Network partition probability gets higher when the value of the distance is increased due to numerous reasons, including but not limited to channel fading and distribution of vehicles. Thus, HERO outperforms BRAVE and MOZO due to the connectivity function that imposes the date packets to be routed through road segments with satisfactory density and shorter distance. Likewise, different from BRAVE and MOZO, our proposed protocol, HERO, rationally utilizes the network's resources through exploiting the vehicles in both directions of the road way, in case of two or more lanes, which surges the packet success ratio, particularly in network with lower density. This is implemented by the two parameters Δ(same direction) and ∇(opposite direction) in Eq.(29). MOZO demonstrates a better success ratio compare to BRAVE. This is because the cluster's header in MOZO interacts with more vehicles, which, in turn, gives MOZO a higher chance to retransmit the date packet before depleting the predefined retransmission attempts.

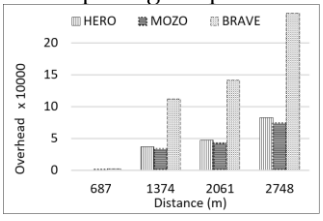

Fig. 11: Communication overhead varying distance.

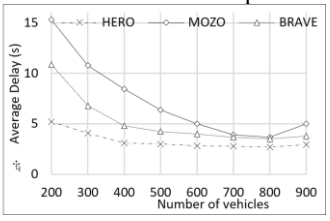

Fig.12: Average delivery latency varying number of vehicles.

(c) Communication Overhead. Fig. 11 presents the simulation results of communication overhead varying different values of distance. It shows that the communication overhead gets greater as the distance from the source vehicle to the destination vehicle increases. This happens due to the necessity of picking more candidate vehicles, and hence more control packets are generated all the way until the data packet arrives its destination. HERO and MOZO incurred similar communication overhead, while BRAVE incurred more overhead since BRAVE first transmits the data packet to the candidate vehicles and then picks up a candidate to further disseminates the data packet towards the destination. HERO shows good performance, nearly equal to the clustered-based protocols due to utilizing the

Neighbors Assortment Eq. (33), which saves the candidate's information based on the score of similarity, which highly reduces the periods of discovering nearby candidate vehicles. MOZO exhibits a smaller communication overhead since the clustered-structure reduces many of control packets during the data dissemination since the members openly contact with the cluster's header, and no need for control packets to discover the next-hop vehicle (candidate vehicle). However, MOZO suffered a lot of overhead for constructing, maintaining, merging, and splitting the moving zones.

6.2.2 Varying Vehicles Number

In this evaluation scenario, vehicles count varies from 200 to 900, from which 100 source vehicles are selected, each source vehicle picks up a destination vehicle within a distance of 2000m, and each source vehicle generates one data packet.

(a) Delivery Latency. Fig. 12 shows the simulation results of latency varying the vehicles count. It shows that a large number of vehicles highly increases the connectivity of the network. This certainly reduces the latency since the *carry-and-forward* times are reduced. With lower density, the vehicles carry the packet multiple times, and also it takes longer for the data packet to be disseminated. Our protocol, HERO, reduces the times of *carry-and-forward,* as it continuously elites the segment that has greater connectivity and a shorter distance, which significantly reduces the chance of a packet to travel via a partitioned road segment. For this reason, HERO attains faster delivery of packets than BRAVE and MOZO. On the contrary, BRAVE and MOZO used *Dijkstra's algorithm* to pick up the road segment with the shortest distance without taking into account the segment connectivity. This seriously consumes the number of *carry-and-forwards* and hence makes the delivery of packets slower.

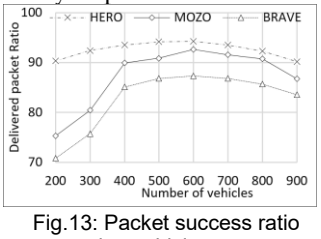

Fig.13: Packet success ratio varying vehicles count.

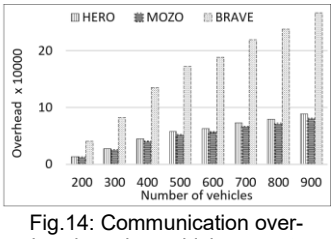

Fig.14: Communication overhead varying vehicles count.

(b) Packet Success Ratio. Fig. 13 shows the simulation results of the packet success ratio varying the vehicles count. It indicates that the delivery rate increases with the count of vehicles then decreases, following a bell curve. As the number of vehicles increases from 200 to 600, the connectivity of the network increases, so the chance of encountering a network partition decreases. This undoubtedly increases the delivery success rate. Also, the results indicated that network connectivity gets higher when the number of vehicles between 700 and 900. But this likely causes channel conflict and may lead to more collisions, so more packets will be dropped. HERO demonstrated a better packet success ratio compared to BRAVE and MOZO. This is partially due to the connectivity function Eq.(26) and the segment length mass function Eq.(22). These two mass functions balanced the traffic jam and network connectivity. In longer road segments, especially when the number of vehicles is large, vehicles may be fairly distributed rather than crowded. In such a case, the packet is better to travel through a longer segment than to travel in a short segment. In HERO, the shortest distance distribution $\widetilde{\Phi}_{i,j}$ is obtained by combining two mass functions, as in Eq. (15), the direction angle $\theta_{i,j}$ and perpendicular distance $\tilde{\psi}_{i,j}$. The direction distribution assigns higher priority for junctions toward the destination, while the perpendicular distance distribution assigns higher priority for junctions that are closer to the centerline between the source and the destination.

(c) Communication Overhead. Simulation results of overhead varying vehicles count are presented in Fig. 14. Obviously, more vehicles in a road segment increase the communication overhead since the candidates in each hop are increased. For clustered-based protocol MOZO, more control packets are generated to maintain the moving zones, which definitely raises the network overhead. Conversely, the overhead in flat-based protocols HERO and BRAVE is increased since more beacon packets are generated (i.e., more candidate vehicles). HERO and MOZO incurred similar overhead, which is lower than the overhead incurred by BRAVE. The detailed reasons for this have been listed so far in the previous sub-section.

6.2.3 Varying Packets Count

We evaluated HERO's performance by varying packets count, namely between 100 and 500 packets. Vehicles count is set by default to 400, while the separation distance from the source vehicle to the destination vehicle is set by default to 2000m. The packets are instantaneously generated at the same moment.

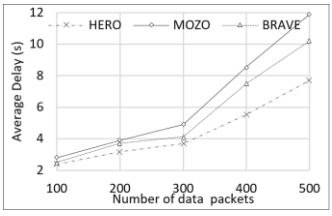

Fig.15: Average delivery latency varying packets count.

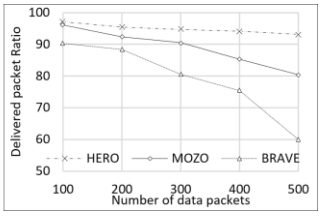

Fig. 16: Packet success ratio varying packets count.

(a) Delivery Latency. Fig.15 shows the simulation results of delivery latency varying the number of packets. BRAVE and HERO showed lower latency than MOZO partially due to the reasons clarified in the previous sub-section. Furthermore, to reduce the queuing delay (i.e., the time a packet waits in the queue until it can be relayed), HERO utilizes the mass function of buffer size (i.e., Eq. (30)**),** which assigns higher priority for the vehicles with more available buffers. The next-hop vehicle in HERO is selected based on the heuristic function Eq.(27), which combines four probability distributions, the speed difference $\tilde{S}_{i,j}$ (Eq.(28)), the direction $\widetilde{\mathcal{D}}_{i,j}$ (Eq.(29)), the available buffer size $\widetilde{\mathcal{M}}_{i,j}$ (Eq.(30)) and the signal fading $\tilde{\mathcal{F}}_{i,j}$ (Eq.(32)). Such quantities are not considered in BRAVE and MOZO.

(b) Packet Success Ratio. Simulation results for packet

success ratio varying the packets count in the network are presented in Fig. 16. More packets in the network certainly consumes the wireless medium and increases the contention. This definitely reduces the success ratio of packets. HERO demonstrated better performance compared to BRAVE and MOZO partially due to the reasons clarified in the previous sub-section.

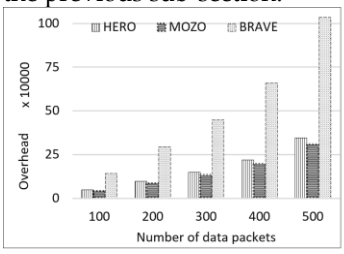

Fig.17: Communication overhead varying packets count.

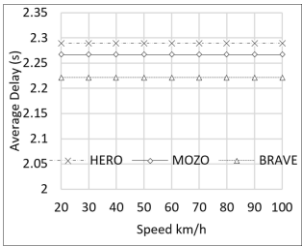

Fig.18: Average delivery latency varying vehicle's speed.

(c) Communication Overhead. Fig.17 shows the simulation results of overhead varying the packets count. It shows that more packets generated in the network definitely rise the overhead partially due to the reasons clarified in the previous sub-section.

6.2.4 Varying Vehicle Speed

In this scenario, the number of vehicles is set to 400 by default. The average speed of vehicles varies between 20 km/h and 100 km/h. For each average speed, 1,000 data packets are generated randomly within 2,000m of the distance. The other parameters are defined as shown in Table 2. As a result, vehicle speed has no significant impact on the delivery delay as shown in Fig.18. However, the average speed has a slight impact on the delivery rate and overhead of the network, as shown in Fig. 19 and Fig. 20, respectively. For a given density, especially when the network is partitioned, the rapid network changes may lead to fast network recovery. This can cause an increase in both the delivery ratio and the network overhead.

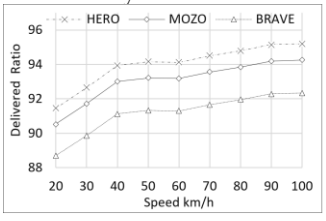

Fig.19: Packet success ratio varying vehicle's speed.

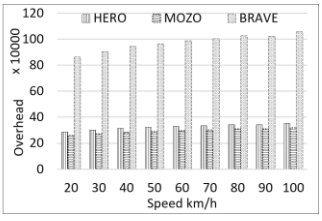

Fig.20: Communication overhead varying vehicle's speed.

7. Conclusion

We presented a distributed routing protocol for the vehicular urban environment, HERO, which comprises two heuristic functions, *Inter-path* and Intra-path, to optimize the selection of road segments and vehicles on road segments, respectively. The *Inter-path* is designed to select a routing path that consists of multiple road segments with a shorter distance and higher connectivity. This is implemented through two probability distributions, namely, the Shortest Distance Distribution (SDD) and the Connectivity Distribution (CD). Each distribution considers multiple quantities that capture the physical property, which enhances the routing decision. SDD considers the direction angle, the perpendicular distance, and segment length while CD considers the communication range, lanes count on the road segment, the length of the segment, and the expected vehicles count. On the other hand, the heuristic function of Intra-path prioritizes vehicles in the road segment based on four routing quantities, speed difference, the vehicle moving direction, buffer size, and signal fading.

Considering the mechanism of multi-criteria routing can highly enhance the performance of VANET, however, two main difficulties are faced during working in this paper. First, how to mathematically model each criterion, while the second difficulty is how to aggregate these conflict criteria in order to obtain an optimal routing decision. Despite HERO supports V2V communication, it can be modified to support V2I communication by allowing the vehicles to hand the packets to roadside units at junctions rather than searching for a forwarder vehicle on other neighbor road segment.

Acknowledgments

This paper is supported by the "Fundamental Research Funds for the Central Universities NO. WK2150110007 and WK2150110012" and by the National Natural Science Foundation of China (NO. 61772490, 61472382, 61472381, 61701322 and 61572454).

References

[1] L. Zhao, A. Al-Dubai, A. Y. Zomaya, G. Min, A. Hawbani and J. Li, "Routing Schemes in Software-Defined Vehicular Networks: Design, Open Issues and Challenges," in IEEE Intelligent Transportation Systems Magazine, doi: 10.1109/MITS.2019.2953557.

[2] Karagiannis, Georgios, et al. "Vehicular networking: A survey and tutorial on requirements, architectures, challenges, standards and solutions." IEEE communications surveys & tutorials 13.4 (2011): 584-616.

[3] Ayoub Alsarhan, Ahmed Al-Dubai, Geyong Min, Albert Y. Zomaya, Mohammad Bsoul, "A New Spectrum Management Scheme for Road Safety in Smart Cities," IEEE Transactions on Intelligent Transportation Systems 19.11(2018): 3496-3506.

[4] Salkuyeh, Mostafa Asgharpoor, and Bahman Abolhassani. "An adaptive multipath geographic routing for video transmission in urban VANETs." IEEE Transactions on Intelligent Transportation Systems 17.10 (2016): 2822-2831.

[5] Atallah, Ribal, Maurice Khabbaz, and Chadi Assi. "Multihop V2I communications: A feasibility study, modeling, and performance analysis." IEEE Transactions on Vehicular Technology 66.3 (2017): 2801-2810.

[6] Kim, Donghyun, et al. "A new comprehensive RSU installation strategy for cost-efficient VANET deployment." IEEE Transactions on Vehicular Technology 66.5 (2017): 4200-4211.

[7] Gubran Al-Kubati, Ahmed Y. Al-Dubai, Lewis M. Mackenzie, Dimitrios P. Pezaros," Stable infrastructure-based routing for Intelligent Transportation Systems." IEEE ICC 2015: 3394-3399.

[8] Zhang, Bo, et al. "Design of analytical model and algorithm for optimal roadside AP placement in VANETs." IEEE Transactions on Vehicular Technology 65.9 (2016): 7708-7718.

[9] Zhang, Fusang, et al. "CBS: Community-Based Bus System as Routing Backbone for Vehicular Ad Hoc Networks." IEEE Transactions on Mobile Computing 16.8 (2017): 2132-2146.

[10] Ding, Yong, and Li Xiao. "SADV: Static-node-assisted adaptive data dissemination in vehicular networks." IEEE Transactions on Vehicular Technology 59.5 (2010): 2445-2455.

[11] Hussein Chour, Youssef Nasser, Hassan Artail, Alaa Kachouh, Ahmed Y. Al-Dubai, "VANET Aided D2D Discovery: Delay Analysis and Performance," IEEE Transactions on Vehicular Technology 66.9 (2017): 8059-8071.

[12] Zhang, Xinming, et al. "A street-centric opportunistic routing protocol based on link correlation for urban vanets." IEEE Transactions on Mobile Computing 15.7 (2016): 1586 - 1599.
[13] Bravo-Torres, Jack Fernando, et al. "Optimizing reactive routing over virtual nodes in VANETs." IEEE Transactions on Vehicular Technology 65.4 (2016): 2274-2294.
[14] Lin, Dan, et al. "MoZo: a moving zone based routing protocol using pure V2V communication in VANETs." IEEE Transactions on Mobile Computing 16.5 (2017): 1357-1370.
[15] Yao, Lin, et al. "V2X Routing in a VANET Based on the Hidden Markov Model." IEEE Transactions on Intelligent Transportation Systems 19.3 (2018): 889-899.
[16] Ruiz, Pedro M., et al. "Brave: Beacon-less routing algorithm for vehicular environments." Mobile Adhoc and Sensor Systems (MASS), 2010 IEEE 7th International Conference on. IEEE, 2010.
[17] Zhang, Xin Ming, et al. "A street-centric routing protocol based on microtopology in vehicular ad hoc networks." IEEE Transactions on Vehicular Technology 65.7 (2016): 5680-5694.
[18] Chuang, Ming-Chin, and Meng Chang Chen. "DEEP: Density-aware emergency message extension protocol for VANETs." IEEE Transactions on Wireless Communications 12.10 (2013): 4983-4993.
[19] Li, Guangyu, Lila Boukhatem, and Jinsong Wu. "Adaptive quality-of-service-based routing for vehicular ad hoc networks with ant colony optimization." IEEE Transactions on Vehicular Technology 66.4 (2017): 3249-3264.
[20] Nizar Alsharif, and Xuemin Shen. "iCAR-II: Infrastructure-Based Connectivity Aware Routing in Vehicular Networks." IEEE Transactions on Vehicular Technology 66.5 (2017): 4231-4244.
[21] Huang, Lijie, et al. "Efficient Data Traffic Forwarding for Infrastructure-to-Infrastructure Communications in VANETs." IEEE Transactions on Intelligent Transportation Systems 19.3 (2018): 839-853.
[22] C. Wu, S. Ohzahata and T. Kato, "Flexible, Portable, and Practicable Solution for Routing in VANETs: A Fuzzy Constraint Q-Learning Approach," in *IEEE Transactions on Vehicular Technology*, vol. 62, no. 9, pp. 4251-4263, Nov. 2013. doi: 10.1109/TVT.2013.2273945.
[23] A. Hawbani, E. Torbosh, W. Xingfu, P. Sincak, L. Zhao and A. Y. Al-Dubai, " Fuzzy-Based Distributed Protocol for Vehicle-to-Vehicle Communication," in *IEEE Transactions on Fuzzy Systems*. (2019), doi: 10.1109/TFUZZ.2019.2957254.
[24] Mezher, Ahmad Mohamad, and Mónica Aguilar Igartua. "Multimedia Multimetric Map-aware Routing protocol to send video-reporting messages over VANETs in smart cities." IEEE Transactions on Vehicular Technology 66.12 (2017): 10611-10625.
[25] Killat, Moritz, and Hannes Hartenstein. "An empirical model for probability of packet reception in vehicular ad hoc networks." EURASIP Journal on Wireless Communications and Networking 2009 (2009): 4.
[26] Ma, Xiaomin, et al. "MAC and application-level broadcast reliability in vanets with channel fading." Computing, Networking and Communications (ICNC), 2013 International Conference on. IEEE, 2013.
[27] Gramaglia, Marco, et al. "New insights from the analysis of free flow vehicular traffic in highways." World of Wireless, Mobile and Multimedia Networks (WoWMoM), 2011 IEEE International Symposium on a. IEEE, 2011.
[28] Panichpapiboon, Sooksan, and Wasan Pattara-Atikom. "Connectivity requirements for self-organizing traffic information systems." IEEE Transactions on Vehicular Technology 57.6 (2008): 3333-3340.
[29] A. Hawbani, X. Wang, L. Zhao, A. Al-Dubai, G. Min and O. Busaileh, "Novel Architecture and Heuristic Algorithms for Software-Defined Wireless Sensor Networks," in IEEE/ACM Transactions on Networking, doi: 10.1109/TNET.2020.3020984.
[30] Hawbani, Ammar, et al. "Zone Probabilistic Routing for Wireless Sensor Networks." IEEE Transactions on Mobile Computing (2018).
[31] Tang, Zhanyong, Yujie Zhao, Lei Yang, Shengde Qi, Dingyi Fang, Xiaojiang Chen, Xiaoqing Gong, and Zheng Wang. "Exploiting wireless received signal strength indicators to detect evil-twin attacks in smart homes." Mobile Information Systems 2017 (2017).
[32] Song, Tao, et al. "A cluster-based directional routing protocol in VANET." Communication Technology (ICCT), 2010 12th IEEE International Conference on. IEEE, 2010.
[33] Rao, Ram Shringar, et al. "A probabilistic analysis of path duration using routing protocol in VANETs." International Journal of Vehicular Technology 2014 (2014).

Ammar Hawbani received the B.S., M.S. and Ph.D. degrees in Computer Software and Theory from the University of Science and Technology of China (USTC), Hefei, China, in 2009, 2012 and 2016, respectively. Currently, he is a postdoctoral researcher in the School of Computer Science and Technology at USTC. His research interests include IoT, WSNs, WBANs, WMNs, VANETs and SDN.

Xingfu Wang received the B.S. degree in electronic and information engineering from Beijing Normal University of China in 1988, and the M.S. degree in computer science from the University of Science and Technology of China in 1997. He is an associate professor in the School of Compute Science and Technology, University of Science and Technology of China. His current research interests include Information Security, Data Management and WSN.

Ahmed ADubai [SM] is Professor of Networking and Communication Algorithms in the School of Computing at Edinburgh Napier University, UK. He received the PhD degree in Computing from the University of Glasgow in 2004. His research interests include Communication Algorithms, Mobile Communication, Internet of Things, and Future Internet. He received several international awards.

Liang Zhao is an associate professor at Shenyang Aerospace University, China. He received his PhD degree from the School of Computing at Edinburgh Napier University in 2011. Before joining Shenyang Aerospace University, he worked as senior associate researcher in Hitachi (China) Research and Development Corporation from 2012 to 2014. His research interests include WMNs, VANETs, and SDN.

Omar Busaileh received his B.S. degree in Electronic and Information Engineering from Hefei University of Technology. Currently he is a Master student in the School of Computer Science and Technology at USTC. His research interests mainly include WSNs, WBANs and SDN.

Ping Liu received his B.S. degree in Computer Science and Technology from Guangdong University of Technology. Currently he is a PhD student in the School of Computer Science and Technology at USTC. His research interests mainly include VANETs, IoT, WSNs, and WMNs.

Mohammed A. A. Al-qaness received the B.S., M.S., and Ph.D. degrees from the Wuhan University of Technology, in 2010, 2014, and 2017, respectively, all in information and communication engineering. He is currently an Assistant Professor with the School of Computer Science, Wuhan University, Wuhan, China. He is also a Postdoctoral Follower with the State Key Laboratory for Information Engineering in Surveying, Mapping, and Remote Sensing, Wuhan University. His current research interests include wireless sensing, mobile computing, machine learning, signal and image processing, and natural language processing.